

Lifetimes and oscillator strengths for Y III

S.T. Maniak¹, L.J. Curtis¹, C.E. Theodosiou¹, R. Hellborg², S.G. Johansson², I. Martinson², R.E. Irving¹, and D.J. Beideck¹

¹ Department of Physics and Astronomy, University of Toledo, Toledo, OH 43606, USA

² Department of Physics, University of Lund, S-223 62 Lund, Sweden

Received 30 September 1993 / Accepted 26 October 1993

Abstract. Lifetime measurements, using beam-foil excitation, are reported for doubly charged yttrium, Y III. The experimental data, for 4d – 5p, 5s – 5p, 5p – 6s and 5p – 5d transitions, are corroborated by new theoretical calculations using the method of Coulomb Approximation with a Hartree–Slater model core (CAHS). The results provide information about Y III transitions observed in HST spectra of Hg–Mn stars.

Key words: atomic data – stars: chemically peculiar

1. Introduction

Absorption lines of neutral and singly ionized yttrium have been observed in spectra of the sun and various stars. An anomalous abundance pattern for the elements Sr–Y–Zr was found in Hg–Mn stars by Guthrie (1971), showing higher Y/Sr and Y/Zr ratios than expected from the s-process of neutron capture. This anomaly has been verified by Adelman (1989) in an extensive abundance analysis of three Hg–Mn stars that was based on more than 50 spectral lines of Sr II, Y II and Zr II in the optical region. Recently, Redfors & Cowley (1993) derived the yttrium abundance from Y III lines observed in IUE spectra of three Hg–Mn stars, ϕ Her, κ Cnc, and ι CrB. An interesting result was that the abundance derived from the Y III lines was higher than that obtained from Y II transitions which Redfors & Cowley interpreted as a departure from LTE for this element. Also in the spectrum of the chemically peculiar star χ Lupi, as observed with the Hubble Space Telescope (HST), two Y III lines have been identified (Leckrone et al. 1993, private communication).

While oscillator strengths for astrophysically significant Y I and Y II transitions have been available for several years (Hannaford et al. 1982, and references therein), very little has been known about gf-values in Y III. To overcome this lack of data, Redfors (1991), using the relativistic Hartree–Fock code of Cowan (1981), presented transition probabilities for a large number of Y III lines.

The structure of Y III – which belongs to the Rb I isoelectronic sequence – is relatively simple, dominated by configurations with one electron outside the closed 4p⁶ subshell. While

the ground term in Rb I and Sr II is 5s²S, the lowest term in Y III is 4d²D. The wavelengths and energy levels of Y III have been thoroughly investigated by Epstein & Reader (1975) who used a sliding spark light source and high-resolution spectrographs.

Thus, the energy level structure of Y III is accurately known and there already exist theoretical data on transition probabilities, but no experimental lifetimes or gf-values have been reported. In order to fill this gap we have now determined lifetimes of low-lying levels in Y III, using the beam-foil excitation method including detailed studies of cascade effects. Parallel with the experimental work we also undertook new calculations of gf-values for Y III.

2. Experiment

The measurements were carried out in the University of Toledo Heavy Ion Accelerator laboratory. The experimental facilities, including the 330 kV ion accelerator and the on-line data analysis systems, have been described in recent literature (Haar et al. 1993; Haar & Curtis 1993). We also refer to papers on lifetimes for levels in C I (Haar et al. 1991), Si IV (Maniak et al. 1993), Au II (Beideck et al. 1993a) and Hg III (Beideck et al. 1993b) which contain fairly detailed descriptions of the experimental procedure and data analyses.

In the present experiment metallic Y filings were introduced into the high temperature oven of the ion source of the accelerator. The discharge was burning on Ar, and by leaking small amounts of CCl₄ the production of Y⁺ ions was facilitated. These ions were accelerated to an energy of 250 keV and directed through a thin (2.4 $\mu\text{g cm}^{-2}$) carbon foil. The radiation emitted by the foil-excited ions was analyzed with an Acton 1 m normal incidence vacuum monochromator, equipped with a 600 l/mm grating blazed at 3000 Å. The photons were detected with a cooled Centronic photomultiplier.

Spectra were registered in the region 2100–3000 Å. The lifetimes were measured in the usual way, by recording the intensity of a given spectral line as a function of the distance (downstream) from the foil. The velocity of the 250 keV Y⁺ ions from the accelerator was known with an uncertainty smaller than 1%. Using semiempirical relations (see Beideck et al. 1993a,b) we estimated the energy loss for these incoming Y⁺

ions to be $5.5 \text{ keV } \mu\text{g}^{-1} \text{ cm}^2$, or 13.2 keV in the foils used. The velocity of the ions after the foil was thereby determined to $0.717 \pm 0.014 \text{ mm ns}^{-1}$. In addition to the velocity loss, the ions also undergo scattering in the foil resulting in a slightly divergent beam on the downstream side, as discussed by Haar et al. (1991). This effect was computed, using available data (for details see Beideck et al. 1993a,b), and corrections were applied in the data analyses.

The ion energy used, 250 keV , is favourable for producing singly and doubly charged Y. Thus, semiempirical calculations (Nikolaev & Dmitriev 1968) predict the following charge distribution after the foil Y (3%), Y^+ (46%), Y^{++} (47%) and Y^{+++} (4%). The Y II spectrum, recently analyzed by Nilsson et al. (1991), is quite line-rich and blending of the Y III lines under study by Y II transitions had to be carefully examined. However, the beam-foil spectra showed convincingly that the Y III transitions of principal interest for the present study were very intense, whereas most of the Y II lines observed were orders of magnitude weaker. In a few cases ($5p-5d$ and $5p-6s$ multiplets in Y III) wavelength coincidences (within our experimental spectral resolution) with Y II lines were possible, but the latter lines have very low intensities (Nilsson et al. 1991). Even significantly stronger Y II lines were barely visible in our beam-foil spectra. Furthermore, we found that the lines of the Y III multiplets $4d \ ^2D - 5p \ ^2P$, $5s \ ^2S - 5p \ ^2P$, $5p \ ^2P - 5d \ ^2D$ and $5p \ ^2P - 6s \ ^2S$ exhibited intensity ratios that were in nearly perfect agreement with the LS-coupling values. We are therefore confident that blending is negligible in the present work. Sections of the spectra are displayed in Fig. 1. The strong Y III multiplets, for which decay measurements were made, are indicated. Most other lines belong to Y II.

Decay curves were recorded for transitions from the levels $5p \ ^2P_{1/2}$, $5p \ ^2P_{3/2}$, $5d \ ^2D_{3/2}$, $5d \ ^2D_{5/2}$ and $6s \ ^2S_{1/2}$. The lifetimes of the $5p$ levels were measured both using transitions to $5s \ ^2S_{1/2}$ and to the $4d \ ^2D_{3/2,5/2}$ ground term, and the results were consistent within 2–3%. Also for the $6s \ ^2S_{1/2}$ and $5d \ ^2D_{3/2,5/2}$ terms, the decay studies involved two lines of each multiplet. The decay curves were initially analyzed with the program DISCRETE (Provencher 1976) which fits the data to a sum of exponentials, representing the lifetime of the level under study and those of higher levels feeding it. If the lifetimes of the primary level and of the higher, cascading levels are close to each other, such a multiexponential fit may lead to considerable uncertainties. A much better method is provided by the technique of arbitrarily normalized decay curves (ANDC), introduced by Curtis et al. (1971), which corrects for cascades in a more rigorous way. The principle of ANDC is briefly as follows:

If the level under study i with a lifetime τ_i is fed from several higher levels j with lifetimes τ_j , the time evolution of the measured intensities $I(t)$ is expressed as

$$dI_i(t)/dt = -I_i(t)/\tau_i + \sum \xi_j I_j(t). \quad (1)$$

Here the quantities ξ_j represent time-independent normalisation constants which take into account transition probabilities, branching ratios, detection efficiencies, etc. Note that a detailed

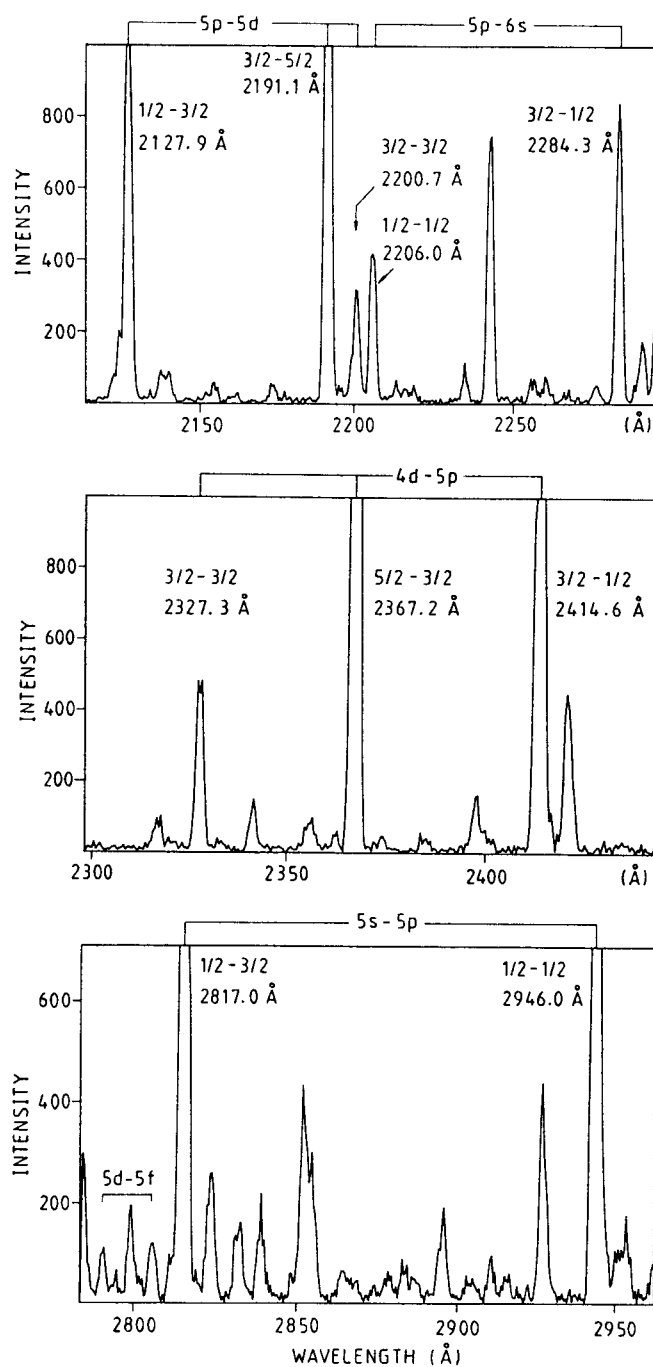


Fig. 1. Examples of beam-foil spectra of Y. The strongest Y III lines are indicated. Most of the other transitions belong to Y II

knowledge of these individual quantities is not necessary. By recording the decays of the primary level i and all the dominant cascading levels j , an overdetermined set of linear equations is obtained which can be solved for the parameters τ_i and ξ_j . Only direct cascades need be measured because indirect cascades, from levels k , that populate i via j , are already included in the measured decay curves $I_j(t)$.

The ANDC method was applied to the $5p \ ^2P$ levels, the decay curves of which were analyzed jointly with those of the $5d \ ^2D$

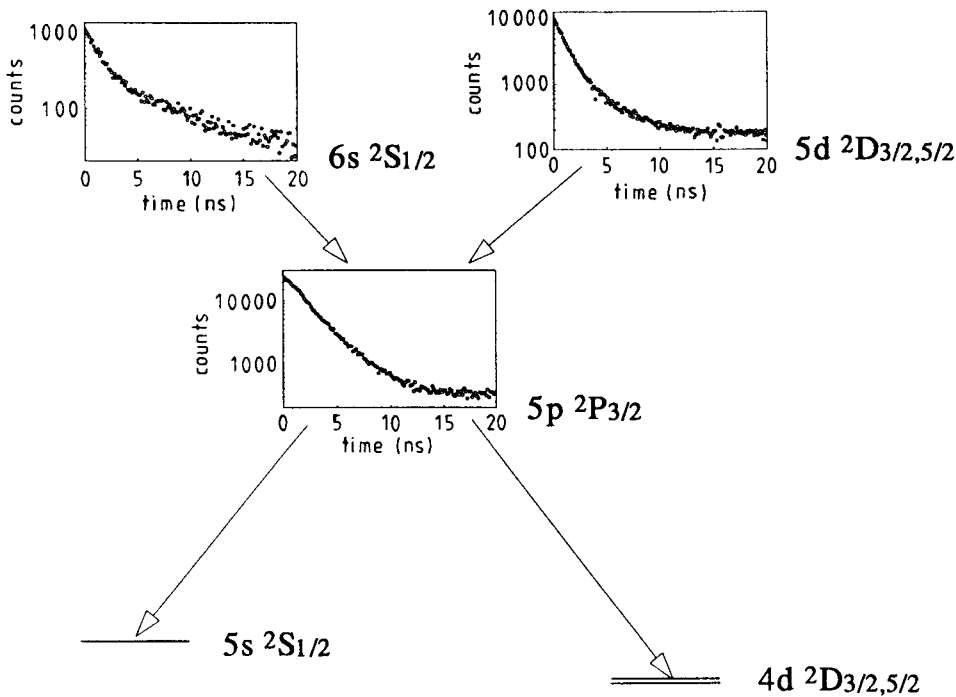


Fig. 2. Decay curves of the $5p \ ^2P_{3/2}$ level and its principal cascades, $6s \ ^2S_{1/2}$ and $5d \ ^2D_{3/2,5/2}$. The decay curves are superimposed on a Grotrian diagram to illustrate their joint analysis by the ANDC method

and $6s \ ^2S$ levels. An example of the decay of $5p \ ^2P_{3/2}$ and its feeding from $6s$ and $5d$ is shown in Fig. 2. The ANDC equations were solved using the computer program CANDY (Engström 1982). The measurements and analysis procedure are similar to those applied by Maniak et al. (1993) to Na-like Si IV.

3. Theoretical calculations

The theoretical approach employed in this work was detailed by Theodosiou (1984). Here we repeat the general features and some refinements. The wavefunctions of the nl states were obtained by the Coulomb Approximation with a central potential core (CACP) method (Theodosiou 1984), i.e. by direct inward integration of the Schrödinger equation

$$\left[\frac{d^2}{dr^2} - V_{lj}(r) - \frac{l(l+1)}{r^2} + E_{nlj} \right] P_{nlj}(r) = 0 \quad (2)$$

where the potential

$$V_{lj}(r) = V_{HS}(r) + V_{pl}(r) + V_{so}(r) \quad (3)$$

consists of the following three terms:

(i) The single-electron central field V_{HS} due to the nucleus and the core electrons, which is calculated within the Hartree–Slater approximation (Herman & Skillman 1963; Desclaux 1969).

(ii) The polarization potential V_{pl} which represents the effect of the induced core electron dipole moment on the active electron, and is taken to be of the form

$$V_{pl}(r) = -\frac{1}{2} a_d r^{-4} \left\{ 1 - \exp \left[- (r/r_{cl})^6 \right] \right\} \quad (4)$$

where the static polarizability a_d was calculated by Johnson et al. (1983). The cutoff distances r_{cl} , are adjustable parameters obtained by iteration so that the “model” potential

$$V_m = V_{HS} + V_{pl} \quad (5)$$

reproduces the experimental binding energies of the lowest energy levels (i.e. $4d$, $5s$ and $5p$) of the active electron. The above adjustments resulted in different values for the core radii r_{cl} for each symmetry l .

(iii) The spin-orbit potential V_{so} is taken to be the term in the Pauli equation, and is given by

$$V_{so}(r) = \frac{1}{2} \alpha^2 \left\{ 1 + (\alpha^2/4) [E - V_m(r)] \right\}^{-2} \times (1/r) \left[dV_m(r)/dr \right] \mathbf{L} \cdot \mathbf{S} . \quad (6)$$

Finally, the necessary radial matrix elements were calculated using the expression

$$\langle nl|r \left(1 - \frac{a_d}{r^3} \left(1 - \frac{1}{2} \left[e^{-(r/r_{cl})^3} + e^{-(r/r_{cl'})^3} \right] \right) \right) |n'l' \rangle \quad (7)$$

similar to the one used by Norcross (1973).

4. Results and discussion

The experimental lifetimes are given in Table 1 where they are compared with theoretical values, by Redfors (1991) and from present Coulomb-approximation calculations. As noted earlier the lifetimes of some levels were measured from two decay channels, and the corresponding transition wavelengths are given in Table 1. For the $5p \ ^2P_{1/2,3/2}$ levels we give the values obtained from the ANDC analyses, 2.06 and 1.79 ns, respectively. These values are quite different from those obtained using optimal fits of the DISCRETE program, 2.40 and

Table 1. Lifetimes of levels in Y III

Upper level	Transition wavelength (Å)	Lifetime (ns)	
		Experiment ^a	Theory
5p ² P _{1/2}	2414.6; 2946.0	2.06 ± 0.08 ^b	2.146 ^d ; 1.52 ^e
5p ² P _{3/2}	2367.2; 2817.0	1.79 ± 0.08 ^b	1.948 ^d ; 1.39 ^e
5d ² D _{3/2}	2127.9	0.93 ± 0.07 ^c	1.098 ^d ; 0.94 ^e
5d ² D _{5/2}	2191.1	1.06 ± 0.08 ^c	1.138 ^d ; 1.01 ^e
6s ² S _{1/2}	2206.0; 2284.3	1.23 ± 0.08 ^c	1.249 ^d 1.23 ^e

^a This work^b Result of ANDC analysis (the difference between ²P_{1/2} and ²P_{3/2} lifetimes is largely caused by the wavelength differences)^c Result of curve-fit, using the DISCRETE program^d This work, Coulomb approximation with a Hartree–Slater core^e Redfors (1991), relativistic Hartree–Fock calculation**Table 2.** gf-values in Y III

Transition	Wavelength (Å) ^a	log gf		
		This work	Redfors (1991)	
5s ² S _{1/2} – 5p ² P _{1/2}	2946.014	–0.204 ^b	–0.187 ^c	–0.07
5s ² S _{1/2} – 5p ² P _{3/2}	2817.037	0.118 ^b	0.154 ^c	0.25
4d ² D _{3/2} – 5p ² P _{1/2}	2414.643	–0.403 ^b	–0.385 ^c	–0.24
4d ² D _{3/2} – 5p ² P _{3/2}	2327.313	–1.099 ^b	–1.060 ^c	–0.92
4d ² D _{5/2} – 5p ² P _{3/2}	2367.228	–0.144 ^b	–0.107 ^c	0.02
5p ² P _{3/2} – 6s ² S _{1/2}	2284.345	–0.079 ^b	–0.073 ^c	–0.09
5p ² P _{1/2} – 6s ² S _{1/2}	2206.029	–0.406 ^b	–0.399 ^c	–0.37
5p ² P _{1/2} – 5d ² D _{3/2}	2127.979	0.318 ^b	0.389 ^c	0.39
5p ² P _{3/2} – 5d ² D _{3/2}	2200.758	–0.373 ^b	–0.301 ^c	–0.33
5p ² P _{3/2} – 5d ² D _{5/2}	2191.159	0.580 ^b	0.610 ^c	0.63

^a Epstein & Reader (1975), air wavelengths^b Coulomb Approximation (CAHS) calculation^c Values based on experimental lifetimes and theoretical (CAHS) branching ratios

2.32 ns, a fact which illustrates that cascading is indeed serious in this case. Of course, this is fairly obvious because the 5p – 6s and 5p – 5d transitions are nearly as intense as the 5s – 5p and 4d – 5p lines in our spectra. Similar findings have been reported in several recent beam-foil studies of lifetimes for ions with one valence electron, see e.g. Maniak et al. (1993), and references therein.

For the 5d and 6s levels we can only report lifetimes based on multiexponential curve fits. However, here the cascading is much less severe than in the case of the 5p levels which implies that our experimental results can be judged to be accurate within 8%. This statement – which assumes that the uncertainty due to cascading does not exceed the uncertainties due to statistics, ion velocity and beam divergence – is based on the following arguments. The 6s ²S level is primarily fed from the 6p and 7p ²P terms for which the theoretical lifetimes are close to 6 ns and 13 ns, i.e. 5–10 times longer than the 6s lifetime. In this case, it

is relatively simple to perform a reliable decomposition of the multiexponential decay curve, in particular because the statistical uncertainties are small. Indeed, the decay curves of the 6s level show a second component of about 8.8 ns, which probably represents a weighted average of the 6p and 7p lifetimes.

Cascading from 6p and 7p should also affect the 5d decay curves, but in this case we must also consider feeding from the 4f and 5f ²F terms (with theoretical lifetimes of 0.65 and 1.1 ns respectively). Here the situation appears to be more serious, because the latter values are very close to our measured lifetimes for the 5d ²D levels, see Table 1. However, our theoretical calculations also show that only 3% of the 4f decay goes to 5d, the dominant decay channel being the 4d ²D ground term. For 5f, the 5d – 5f branching ratio is calculated to be 15%, but here our spectra show that the 5d – 5f lines (2791.4 and 2806.9 Å) are quite weak, as can be seen from Fig. 1. This is consistent with our earlier results, i.e. that in beam-foil spectra of heavy ions at low energies, low-lying levels are predominantly populated (Beideck et al. 1993a,b). This fact has previously been elaborated upon by Andersen et al. (1979) and Kemmler et al. (1991).

Table 1 shows that the ANDC lifetimes for the 5p levels are in very good agreement with our Coulomb approximation data, but they are about 25% longer than the values reported by Redfors (1991). This discrepancy is somewhat surprising. One possible explanation would be given by core-polarization effects, the omission of which from the theoretical calculations may yield gf-values that are significantly too high (Migdalek 1978). In the case of the Coulomb approximation method, this effect is explicitly included in the calculations. (The contributions to the dipole transition moment due to the polarization of the electron and that of the core tend to cancel, thus reducing decay rates, Hameed et al. 1968.) On the other hand, theory and experiment tend to agree quite well for the lifetimes of the 6s and 5d levels – in these cases the core polarization effects are markedly smaller.

By combining our measured lifetimes with branching ratios calculated by means of the CAHS method, we can obtain “experimental” gf-values. These are listed in Table 2, together with the results of the present calculation and the theoretical data obtained by Redfors (1991). A comparison confirms that the three sets of data agree quite well for the 5p – 5d and 5p – 6s lines, whereas the experimental oscillator strengths are lower than the values obtained by Redfors (1991) for the transitions from 5p levels, by 20–23% (5s – 5p) and 25–28% (4d – 5p). To further clarify this problem, measurements of branching ratios for Y III will be undertaken in Lund.

Acknowledgements. We are grateful to Dr. D.S. Leckrone and Dr. A. Redfors for valuable discussions. Two of the authors (RH and IM) acknowledge the hospitality extended to them at the Department of Physics, University of Toledo and the travel support obtained from the Royal Physiographical Society in Lund. LJC and STM were supported by the U.S. Department of Energy, Office of Basic Sciences, Division of Chemical Sciences.

References

- Adelman S.J., 1989, MNRAS 239, 487
Andersen T., Eriksen P., Poulsen O., et al., 1979, Phys. Rev. A 20, 2621
Beideck D.J., Curtis L.J., Irving R.E., et al., 1993a, J. Opt. Soc. Am. B 10, 977
Beideck D.J., Curtis L.J., Irving R.E., et al., 1993b, Phys. Rev. A 47, 884
Cowan R.D., 1981, The Theory of Atomic Structure and Spectra, University of California Press, Berkeley
Curtis L.J., Berry H.G., Bromander J., 1971, Phys. Lett. 34A, 169
Desclaux J.P., 1969, Comp. Phys. Comm. 1, 216
Engström L., 1982, Nucl. Instr. Methods 202, 369
Epstein G.L., Reader J., 1975, J. Opt. Soc. Am. 65, 310
Guthrie B.N.G., 1971, AP&SS 10, 156
Haar R.R., Curtis L.J., Kvale T.J., et al., 1991, A&A 241, 321
Haar R.R., Beideck D.J., Curtis L.J., et al., 1993, Nucl. Instr. Meth. Phys. Res. B79, 746
Haar R.R., Curtis L.J., 1993, Nucl. Instr. Meth. Phys. Res. B79, 782
Hameed S., Herzenberg A., James M.G., 1968, J. Phys. B 1, 822
Hannaford P., Lowe R.M., Grevesse N., et al., 1982, ApJ 261, 736
Herman F., Skillman S., 1963, Atomic Structure Calculations, Prentice Hall, Englewood Cliffs
Johnson W.R., Kolb D., Huang K.-N., 1983, At. Data. Nucl. Data Tables 28, 333
Kemmler J., Burgdörfer J., Reinhold C.O., 1991, Phys. Rev. A 44, 2993
Maniak S.T., Träbert E., Curtis L.J., 1993, Phys. Letters A 173, 407
Migdalek J., 1978, J. Quant. Spectrosc. Radiat. Transfer 20, 81
Nikolaev V.S., Dmitriev I.S., 1968, Phys. Lett. 28A, 277
Nilsson A.E., Johansson S., Kurucz R.L., 1991, Physica Scripta 44, 226
Norcross D.W., 1973, Phys. Rev. A 7, 606
Provencher S.W., 1976, J. Chem. Phys. 64, 2772
Redfors A., 1991, A&A 249, 589
Redfors A., Cowley C.R., 1993, A&A 271, 273
Theodosiou C.E., 1984, Phys. Rev. A 30, 2881